Journal of Mines, Metals and Fuels, 71(1): 113-120; 2023. DOI: 10.18311/jmmf/2023/33367

Print ISSN : 0022-2755

Journal of Mines, Metals and Fuels

Contents available at: www.informaticsjournals.com/index.php/jmmf

A Numerical Study of Two-Phase Flow Through an Asymmetric Channel with Velocity Slip and Joule Heating Effects

S.H C.V. Subba Bhatta*, S. Ram Prasad and Y. S. Kalyan Chakravarthy

*Department of Mathematics, M. S. Ramaiah Institute of Technology, Bangalore 54, India. *Email: shcvsb@gmail.com*

Abstract

The goal of the current investigation is to examine the impact of velocity slip and Joule heating effects on a particulate flow through an asymmetric channel (convergent channel). The transformed governing equations are solved by employing the shooting method. The impact of influential parameters on fluid as well as particle phases of velocity and temperature fields has been analyzed graphically. The present results exactly match previously published results in some limited cases. In this study, it is perceived that an augmentation in velocity slip leads to an increment in fluid velocity in the left half and a diminution in the right half of the channel.

Keywords: *Particulate suspension, convergent channel, velocity slip, Joule heating*

1.0 Introduction

Flow through oblique walled channels has gained much importance in distinct fields like gas compressors, fibre manufacturing, metal casting, etc. Terril[1] was able to precisely solve the problem of analysing the flow between non-parallel walls. Yilmaz et al[2] have done extensive research on channel flow with slanted walls. Esmaeilpour et al[3] discussed the flow in an asymmetric channel with suction and injection Copper and graphene oxide hybrid nanofluid flow in non-uniform tubes was explored numerically by Hafeez et.al[4]. In this investigation, they noticed an increase in Reynolds number along with an intensification in the velocity. The spectral quasi linearization method was used by Mallikarjuna et.al.[5] to analyse the heat transfer properties of nanofluids in a slanting channel by taking into account stretching and shrinking, Biswal et al.[6] investigated numerically the nanofluid flow between slanting channels.

The suspension of tiny particles in various fluids has become increasingly important in technology recently. These kinds of flows can be seen in the sedimentation of erythrocytes, the cooling effects of air conditioning, etc. Ramprasad et al.[7] used the shooting method to investigate the impact of a magnetic field on particle movement. The effect of radiation on particulate Casson fluid through the non-uniform surface was discussed by Sadia et al.[8]. Using a plate with wavy borders and a time-dependent buoyancy-driven dusty Casson fluid, Hady et al.[9] conducted a numerical investigation. Turkimazoglu[10] explored numerically the heat transfer analysis of particulate flow over a disk. The finite difference method was used by Hosam and Mahdy[11] to examine the dusty micropolar fluid's cone-shaped heat transfer properties. A numerical exploration by Mallikarjuna et al.[12] to discuss the impact of radiation on buoyancy-driven particulate fluid flow in a diverging channel. By taking into account various pressure gradients, Rajesh Kumar et al.[13] were able to arrive at the numerical solution of unstable two-phase flows in channels.

**Author for correspondence*

Slip boundary conditions are useful for transport process of food stuff, optical coatings, the reduction of friction, etc. To discuss the slip effects on oblique walled channels, Ramprasad et al.[14] came up with a numerical solution. The effect of radiation on particle flow in a channel was clearly described by Mallikarjuna et al.[15]. Ohmic heating is highly useful in seawater desalination, incandescent light bulbs, water distillation and food industry etc. Srinivasacharya and Jagadeeshwar[16] implemented the collocation method to study the influence of joule heating in boundary layer. Chamkha et al.[17] implemented the Duan-Rach approach to obtain a solution for hybrid nanofluid flow over parallel surfaces. In this study it is concluded that escalating values of the rotation parameter diminish the velocity of fluid. Swain et al.[18] succeeded in obtaining an analytical as well as numerical solution to investigate ohmic dissipation effects on a sheet. By taking joule heating into account, Umair et al.[19] were able to arrive at a numerical solution to compare the analytical solution for nanofluid flow in an asymmetric channel. Asha and Namrata[20] adopted the homotopy perturbation Sumudu transformation method to analyse the heat transfer effects in a non-uniform channel. Khashi et al.[21] deliberated numerically hybrid nanofluid flow through a disk with suction and injection.

From the above cited literature, one can confirm that no one tried to investigate the particulate flow in a channel with non-parallel walls by considering slip effects and joule heating. The goal of the present investigation is to study the influence of velocity slip and ohmic heating on particulate flow through an asymmetric convergent channel. A numerical solution is obtained using the RK-4 method with the aid of shooting technique. The influence of pertinent parameters on velocity and thermal profiles for both phases is analysed graphically.

2.0 Problem Definition

The flow of incompressible hydromagnetic particles suspended in a fluid via an asymmetric diverging channel is modelled as a viscous, continuous, two-dimensional flow. Figure 1 shows where the channel walls are located. At different walls, varying suction/injection velocities are anticipated. The temperature Tw of the channel walls is kept constant. Normal application of a strong magnetic field H_0 is made to the walls. First order velocity slip and ohmic heating are also taken into consideration.

The governing equations are [7,15]

Fluid phase

$$\frac{\partial}{\partial r}\left(r\overline{U}\right)+\frac{\partial \overline{V}}{\partial \theta}=0 \qquad \text{... (1)}$$

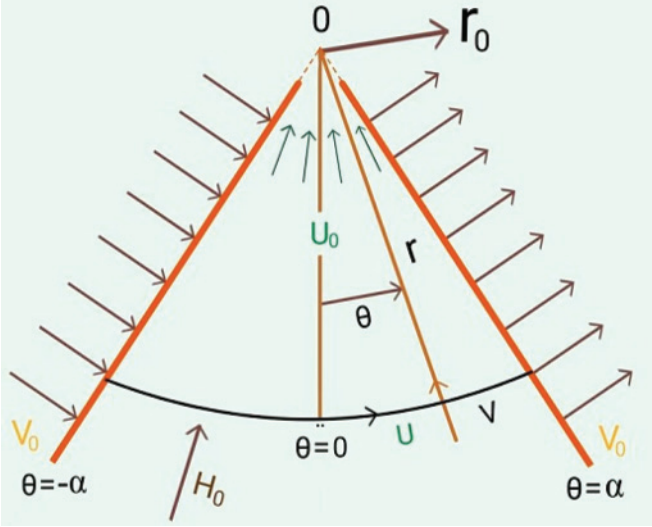

Figure 1: Flow sketch

$$\rho\left(\overline{U}\frac{\partial \overline{U}}{\partial r}+\frac{\overline{V}}{r}\frac{\partial \overline{U}}{\partial \theta}-\frac{\overline{V}^2}{r}\right)=-\frac{\partial p}{\partial r}$$
$$+\mu\left[\left(\frac{\partial^2 \overline{U}}{\partial r^2}+\frac{1}{r}\frac{\partial \overline{U}}{\partial r}+\frac{1}{r^2}\frac{\partial^2 \overline{U}}{\partial \theta^2}\right)-\frac{\overline{U}}{r^2}+\frac{2}{r^2}\frac{\partial \overline{V}}{\partial \theta}\right] \qquad \text{... (2)}$$
$$+\frac{\rho_p}{\rho}S(\overline{U}_p-\overline{U})-\sigma {H_0}^2{\mu_e}^2\overline{U}$$

$$\rho\left(\overline{U}\frac{\partial \overline{V}}{\partial r}+\frac{\overline{V}}{r}\frac{\partial \overline{V}}{\partial \theta}-\frac{\overline{U}\overline{V}}{r}\right)=\frac{-1}{r}\frac{\partial p}{\partial \theta}$$
$$+\mu\left[\left(\frac{\partial^2 \overline{V}}{\partial r^2}+\frac{1}{r}\frac{\partial \overline{V}}{\partial r}+\frac{1}{r^2}\frac{\partial^2 \overline{V}}{\partial \theta^2}\right)-\frac{\overline{V}}{r^2}+\frac{2}{r^2}\frac{\partial \overline{U}}{\partial \theta}\right] \qquad \text{... (3)}$$
$$+\frac{\rho_p}{\rho}S(\overline{V}_p-\overline{V})$$

$$\rho c_p\left(\overline{U}\frac{\partial T_1}{\partial r}+\frac{\overline{V}}{r}\frac{\partial T_1}{\partial \theta}\right)=k\left[\frac{1}{r}\frac{\partial}{\partial r}\left(r\frac{\partial T_1}{\partial r}\right)+\frac{1}{r^2}\frac{\partial^2 T_1}{\partial \theta^2}\right]$$
$$+Q_0T_1+\frac{\rho_p c_m}{\tau_T}(T_{1p}-T_1)+\sigma {H_0}^2{\mu_e}^2\overline{U}^2 \qquad \text{... (4)}$$

Phase II

$$\frac{\partial}{\partial r}(r\overline{U}_p)+\frac{\partial}{\partial \theta}(\overline{V}_p)=0 \qquad \text{... (5)}$$

$$\overline{U}_p\frac{\partial \overline{U}_p}{\partial r}+\frac{\overline{V}_p}{r}\frac{\partial \overline{U}_p}{\partial \theta}-\frac{\overline{V}_p^2}{r}=\frac{-1}{\rho_p}\frac{\partial p}{\partial r}+S(\overline{U}-\overline{U}_p) \qquad \text{... (6)}$$

$$\overline{U}_p\frac{\partial \overline{V}_p}{\partial r}+\frac{\overline{V}_p}{r}\frac{\partial \overline{V}_p}{\partial r}+\frac{\overline{U}_p\overline{V}_p}{r}=\frac{-1}{\rho_p}\frac{\partial p}{\partial \theta}+S(\overline{V}-\overline{V}_p) \qquad \text{... (7)}$$

$$\overline{U}_p \frac{\partial T_P}{\partial r} + \frac{\overline{V}_p}{r}\frac{\partial T_p}{\partial \theta} = \frac{1}{\tau_T}(T_1 - T_{1p}) \quad \ldots (8)$$

The boundary conditions are

$$\overline{U} = -s1\frac{\partial \overline{U}}{\partial \theta}, \overline{U}_p = 0 \text{ at } \theta = \pm\alpha, \overline{U}(r_0, 0) = -u_0$$
$$T_1 = T_w, T_{1p} = T_{wp} \text{ at } \theta = \pm\alpha \quad \ldots (9)$$

Non dimensional equations are

$$f''' + 2\,\mathrm{Re}\; ff' - f'' + L\beta(F' - f') + \left(4 - M^2\right)f' = 0 \quad \ldots (10)$$

$$F'' - 2\frac{\mathrm{Re}}{R}FF' - \frac{\beta}{R}(f' - F') = 0 \quad \ldots (11)$$

$$t'' - R\,\mathrm{Pr}\,t' + \mathrm{Pr}\,Qt + L\beta_t\gamma\,\mathrm{Pr}(T - t) + \mathrm{Pr}\,M^2 f^2 = 0 \quad \ldots (12)$$

$$T' - K(t - T) = 0 \quad \ldots (13)$$

Associated boundary conditions are

$$f(\theta) = -\xi f'(\theta), f(0) = -1,\ F(\pm\alpha) = 0, t(\pm\alpha) = 1,\ T(\pm\alpha) = 1 \quad \ldots (14)$$

Skin friction Coefficient and Nusselt Number

Skin friction $= C_f = \dfrac{\tau_s}{\rho\overline{U}_0^2} = \dfrac{\mu\left(\dfrac{\partial \overline{U}}{r\partial\theta}\right)_{\theta=\pm\alpha}}{\rho\overline{U}_0^2}$; Nusselt number

$$= Nu = \frac{rq_s}{kT_w} = \frac{r\left(\dfrac{-k\partial T_1}{r\partial\theta}\right)_{\theta=\pm\alpha}}{kT_w}$$

In non-dimensional form

$$C_f = \frac{1}{\mathrm{Re}}f'(\pm\alpha) \text{ and } Nu = -t'(\pm\alpha)$$

Code validation

Table 1: Comparison results of skin friction coefficient for M=0, N=0, Gr=0, Pr=0, $\xi = 0, \beta = 1, \beta_t = 0$, k=0 and $\alpha = \frac{\pi}{6}$.

R	Re	Ramprasad et al. [7]		Present Results	
		c_f at $-\alpha$	c_f at α	c_f at $-\alpha$	c_f at α
1	1	–3.01181	4.40237	–3.011034	4.40176
	3	–3.23754	4.58254	–3.23687	4.58216

3.0 Results and Discussion

This section dedicated to discuss how emergent parameters might affect particle phases as well as fluid velocity and temperature distributions. By using the shooting method, the altered equations (10) to (13) with (14) are solved. For calculation purpose, the fixed values M=0.5, L=0.5, Re=0.5, R=0.5, Pr =0.71, Q=0.5, $\alpha = \frac{\pi}{6}$, ξ = 0.5. Changes in velocity profiles due to increment in M are expounded in Fig.2(a). An improvement in M leads to an enhancement in velocity in the left part and a diminishment in the counterpart. But the particle velocity shoots up as elucidated in Fig.2(b). From Fig.3(a) it is clear that as M improves, the temperature profiles get enhanced. Fig.3(b) reveals that the particle temperature rises in 70% and decrease in the remaining part of the channel. It is evident from Fig.4(a) as R increases the fluid velocity magnified in the left half and drops in the right half. But pronounced incline in the particle velocity is noted as sketched in the Fig.3(b). For higher values of R, the fluid temperature drops as reflected in the Fig.5(a). But a complete opposite nature is observed for the particle temperature, as portrayed in Fig.5(b).

An increment in Re leads to a drop in the velocity in the first part, indicating the dominance of viscous forces, and an enhancement in the velocity in the second half which shows the dominance of inertial forces as reflected in the Fig.6(a). But particle velocity drastically diminishes as depicted in the Fig.6(b). Fig.7(a) manifests the impact of ξ on f. An amplification in f is discerned in the left half and a diminution in f is discerned in the right half. Particle velocity rises in the complete channel as shown in the Fig.7(b). From the Fig.8(a) it is clear that the large values of Pr cause an increment in t. The particle temperature improves in 60% and drops in the remaining part of the channel. It is articulate from Fig.9(a) higher values of Q escalate the fluid temperature. From the Fig.9(b) it is perceived that as Q enlarges the particle temperature shoots up in the first half and gradually declines in the second half.

As R, ξ, α improves C_f boost up at the left wall and drops at the right wall. An increment in M drops C_f at the left boundary and improves at the right boundary. An augmentation in R and M surges Nu on both walls. An enlargement in Q and Pr dwindles the Nu on the left wall and rises on the right wall of the channel.

Graphs (Fig.2 to 9)

4.0 Concluding Remarks

The current investigation focused on the effects of velocity slip and ohmic heating on the flow of particulates via an asymmetric convergent channel. The important findings are :

- The temperature and velocity profiles of the particle phase improve as R grows, despite the temperature of the fluid lowers as R rises.
- Both the fluid temperature and particle velocity dramatically increase as M increases.
- As the velocity slip parameter improves, fluid velocity rises in the left part of the channel and falls in the right.
- As Pr values rise, fluid temperature rises, whereas particle

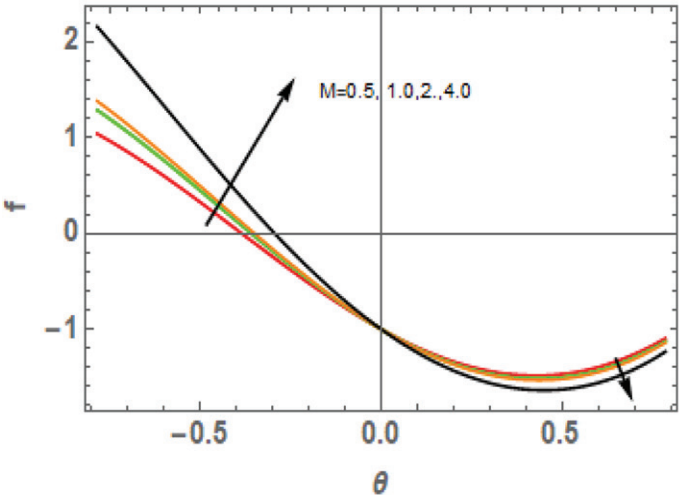

Figure 2: (a) Assesment of M on f

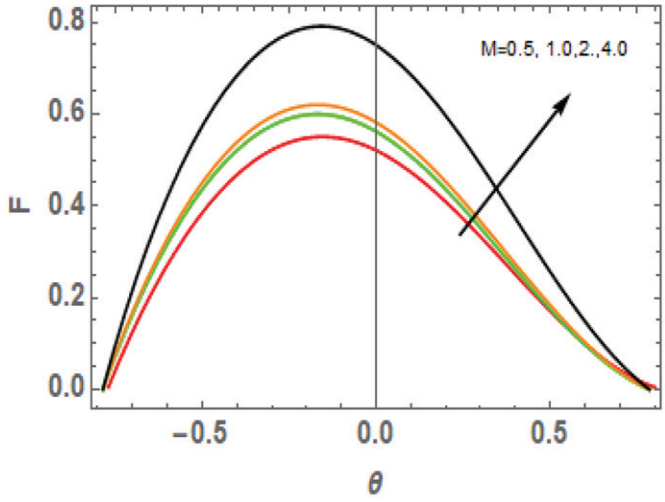

(b) Assesment of M on F

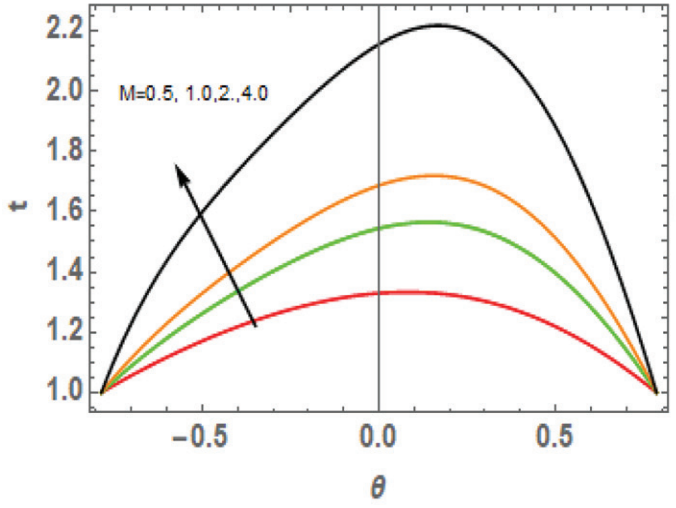

Figure 3: (a) Assesment of M on t

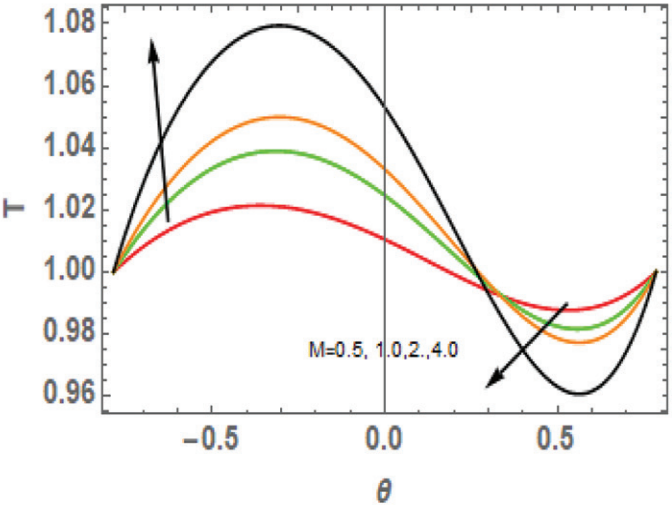

(b) Assesment of M on T

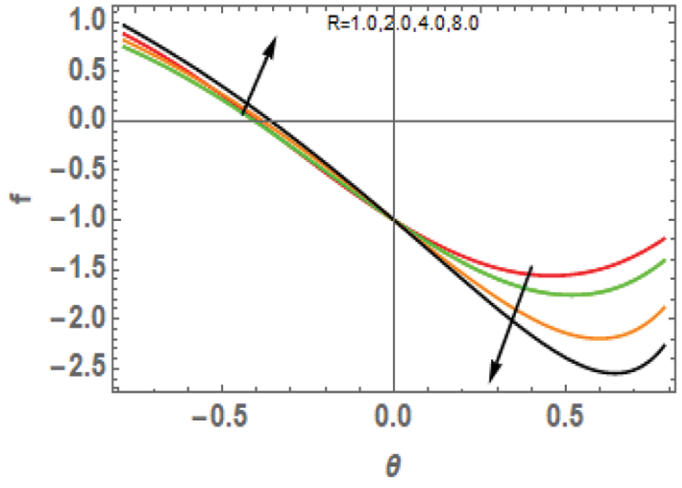

Figure 4: (a) Assesment of R on f

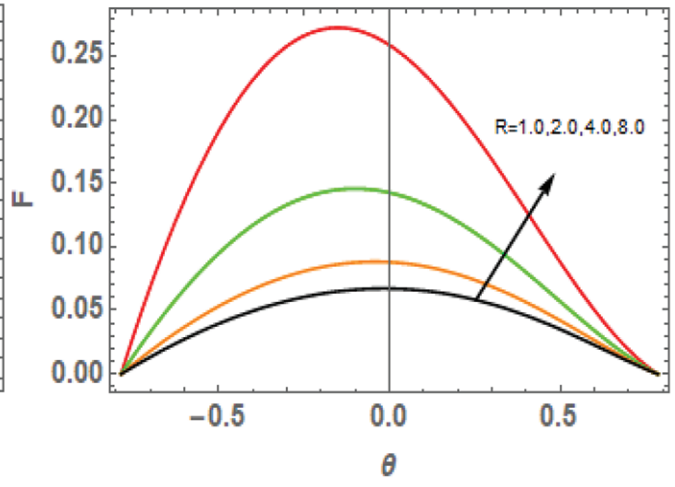

(b) Assesment of R on F

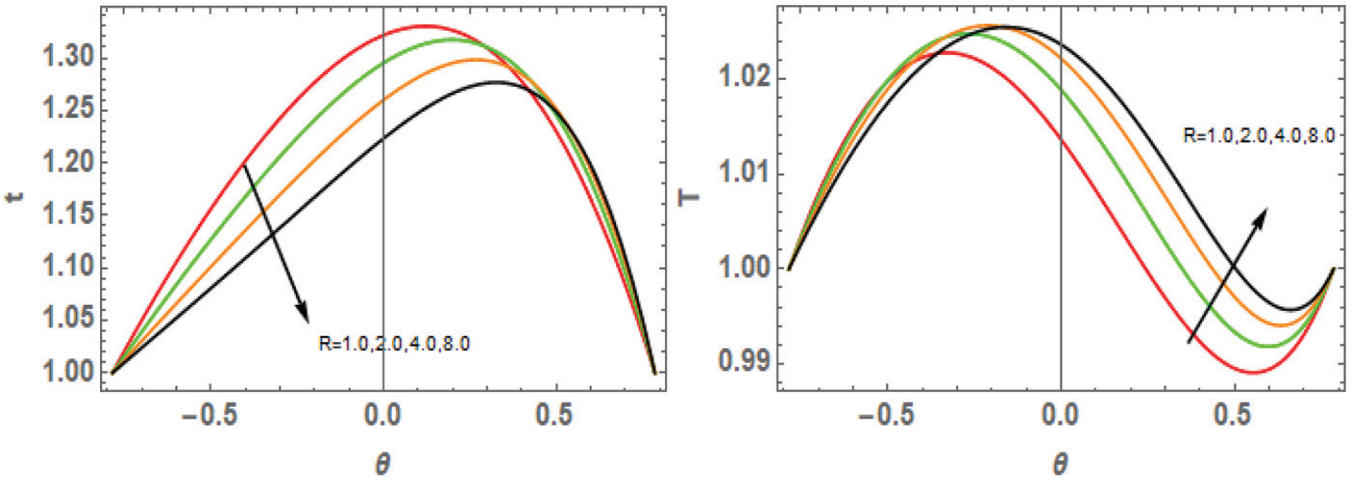

Figure 5: (a) Assesment of R on t (b) Assesment of R on T

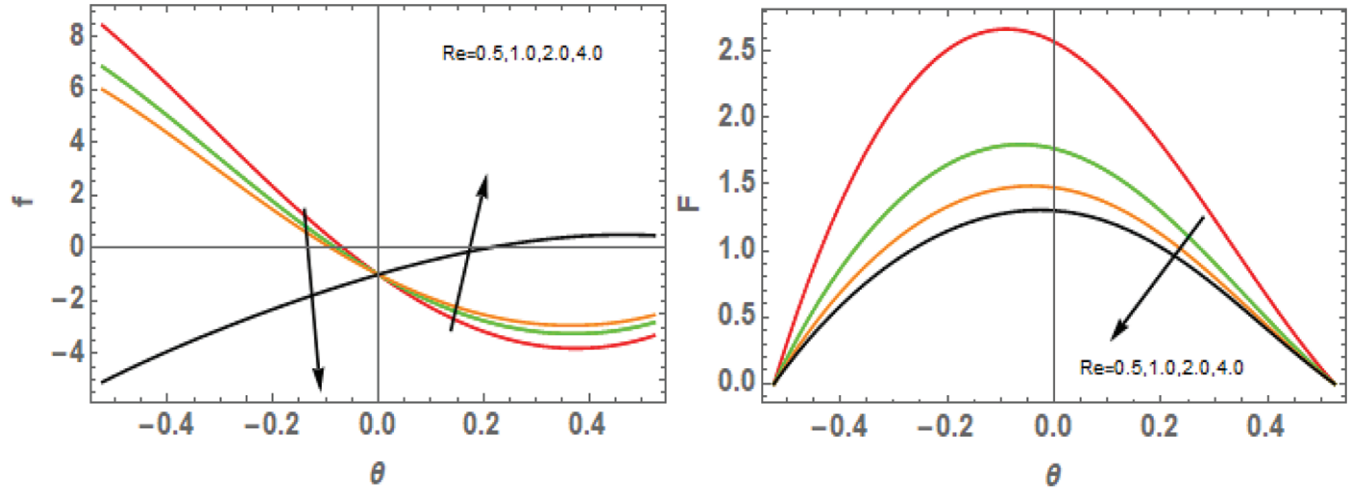

Figure 6: (a) Assesment of Re on f (b) Assesment of Re on F

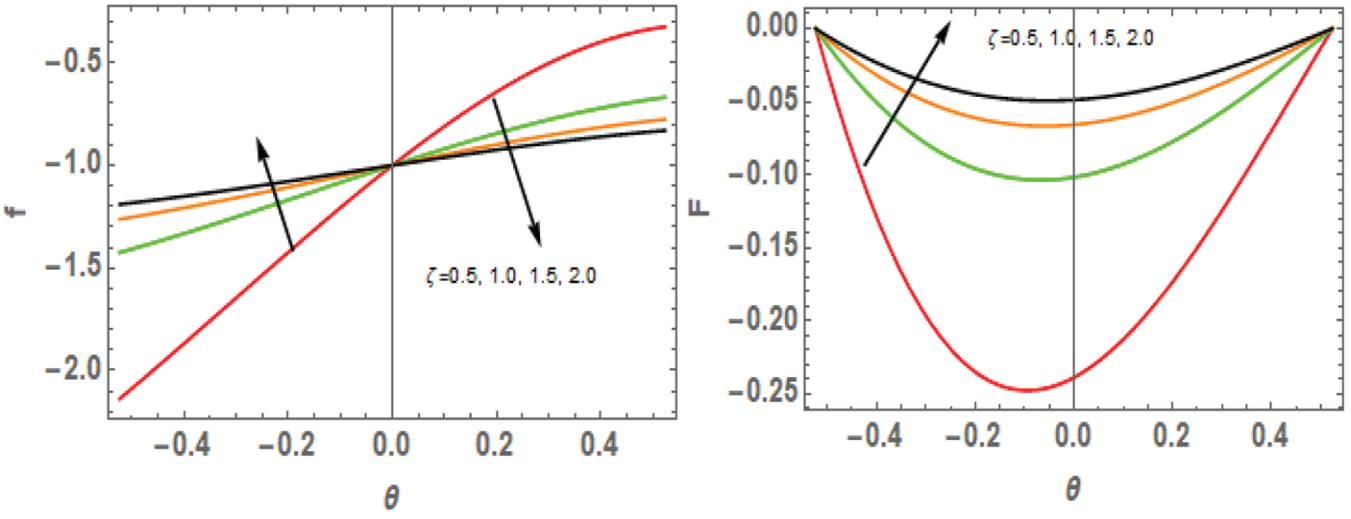

Figure 7: (a) Assesment of ξ on f (b) Assesment of ξ on F

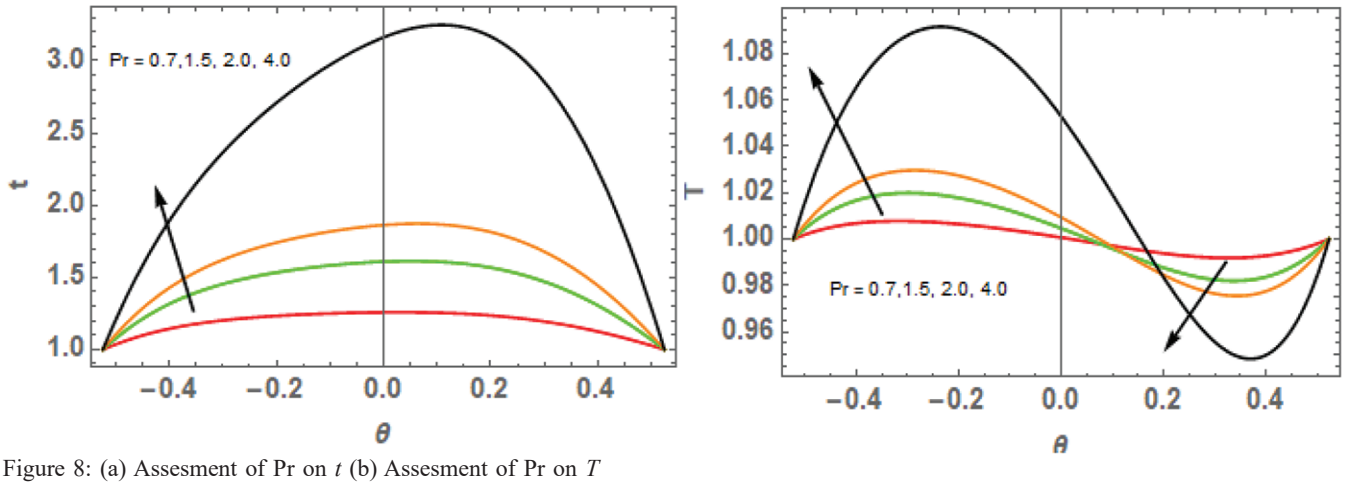

Figure 8: (a) Assesment of Pr on t (b) Assesment of Pr on T

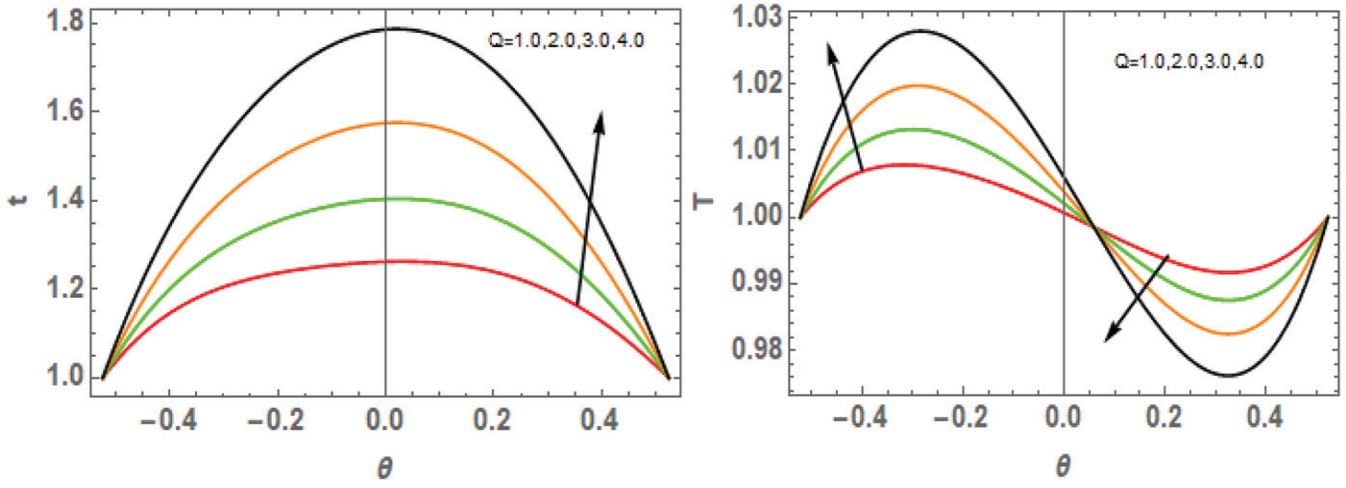

Figure 9: (a) Assesment of Q on t (b) Assesment of Q on T

Table 2: Skin friction and Nusselt number for various values of R, Re, M and L

R	Re	M	L	C_f at $-\alpha$	C_f at α	Nu at $-\alpha$	Nu at α
0.5	0.5	0.5	0.5	-2.08296	2.19176	-0.69263	0.95789
1.0				-1.75694	2.37401	-0.60943	1.05314
2.0				-1.49614	2.81673	-0.46823	1.23585
4.0				-1.62984	3.76677	-0.28316	1.52498
	1.0			-2.31471	2.15482	-0.69742	0.95264
	2.0			-1.89643	2.64194	-0.60057	1.02110
	4.0			-1.59876	2.96764	-0.54317	1.32156
		1.0		-4.64768	3.81476	-0.98674	1.76754
		2.0		-5.17693	3.98676	-0.89674	2.17947
		4.0		-8.16914	4.32671	-0.78674	3.84321
			1	-3.14765	3.09671	-0.19476	1.13476
			1.5	-4.96784	3.47654	-0.19384	1.13476

Table 3: Skin friction and Nusselt number for various values of α, Q, Pr and δ

ξ	Q	Pr	α	C_f at $-\alpha$	C_f at α	Nu at $-\alpha$	Nu at α
0.5	0.5	0.71	$\pi/6$	-1.69874	5.67896	-0.56430	0.85436
1.0				-1.53474	5.13456	-0.56430	0.85436
1.5				-1.49174	4.99343	-0.56430	0.85436
2.0				-1.05143	4.76342	-0.56430	0.85436
	1.0			-3.47695	3.89643	-1.34176	1.47681
	1.5			-3.47695	3.89643	-2.11670	2.31043
	2.0			-3.47695	3.89643	-2.68764	3.11075
		1.5		-2.91473	3.46464	-0.86794	0.89643
		2.0		-2.91473	3.46464	-0.96543	1.69543
		3.0		-2.91473	3.46464	-1.35479	2.79564
			$\pi/5$	-1.68475	6.58430	-0.56430	0.85436
			$\pi/4$	-1.23411	6.13631	-0.56430	0.85436
			$\pi/3$	-0.89472	5.45345	-0.56430	0.85436

temperature rises in the left portion of the channel and declines in the right. Similar trends can be seen in the heat source parameter.

- The Nu on the channel's left wall declines as a result of an expansion in Q and Pr, while the Nu on the right side rises.

5.0 References

1. Terril R.M, (1965): "Slow Laminar Flow in a Converging or Diverging Channel with Suction at One Wall and Blowing at the Other Wall", *ZAMP*, 16,306.
2. Yilmaz, Adil Akyatan and Erol Senocak (1998): "Slow flow of a Reiner-Rivlin fluid in a converging or diverging channel with suction and injection", *Turkish Journal of Engineering and Environmental Sciences*, 27, 179-183.
3. Esmaeilpour, Naeem Roshan, Negar Roshan and Ganji D D, (2011): "Analytical method in solving flow of viscoelastic fluid in a porous converging channel", *International Journal of Mathematics and Mathematical Sciences,* 257903.
4. Muhammed Hafeez, Hashim and Masood khan, (2020): "Jeffrey-Hamel flow of hybrid nanofluids in convergent and divergent channels with heat transfer characteristics", *Applied Nanoscience*, 12, 5459-5468.
5. Mallikarjuna.B, Ramprasad. S, Shezahad S and Ayyaz. R, (2022): "Numerical and regression analysis of Cu nanoparticles flows in distinct base fluids through a symmetric non-uniform channel", *The European Physical Journal Special Topics*, 231,557-569.
6. Uddhab Biswal, Chakraverty. S, Ojha B K, Ahmed Kadhim Hussein, (2022): "Numerical investigation on nanofluid between two inclined stretchable walls optimal Homotopy analysis method", *Journal of Computer Science*, 63, 101759.
7. Ramprasad S, Subba Bhatta S.H.C.V, Mallikarjuna B and Srinivasacharya D, (2017): "Two-phase particulate suspension flow in convergent and divergent channels: A Numerical Model", *International Journal of Applied and Computational Mathematics,* 3, 843-858.
8. Sadia Siddiqaa, Naheed Begum, Anwar Hossanic, Shoabia. M and Rama Subba Reddy. G, (2018): "Radiative heat transfer analysis of non-Newtonian dusty Casson fluid along a complex wavy surface", *Nuerical Heat Transfer,* Part A, 73, 209-221.
9. Hady. F.M, Mahdy.A, Mohammed S.E, Omoma and Abo Zaid, (2019): "Unsteady natural convection flow of a dusty non-Newtonian Casson fluid along a vertical wavy plate: Numerical approach", *Journal of Brazilian Society of Mechanical Sciences and Engineering*, 41, 472.
10. Turkyimazoglu. M, (2020): "Suspension of dust particles over a stretchable rotating disk and two-phase heat transfer", *International Journal of Multiphase Flow,* 127, 103260.
11. Hosam A. Nabwey and Mahdy, (2021): "Numerical approach of micropolar dust-paricles natural convection fluid flow due to a permeable cone with nonlinear temperature", *Alexandria Engineering Journal*, 60, 1739-1749.

12. Mallikarjuna.B, SubbaBhatta. S.H.C.V and Ramprasad. S, "Velocity and thermal effects on MHD convective radiative two-phase flows in an asymmetric non-uniform channel", Propulsion and Power Research, (2021), 10, 169-179.
13. Rajesh Kumar Chandrawat, Varun Joshi and Beg O.A, (2022): "Numerical study of time dependent flow of immiscible Saffman dusty (fluid-particle suspension) and Eringen micropolar fluids in a duct with a modified cubic B-spline Differential Quadrature method", International Communications in Heat and Mass Transfer, 130, 105758.
14. Ramprasad S, Subba Bhatta S.H.C.V and Mallikarjuna B, (2018): "Slip effects on MHD convective Two - phase flow in a divergent channel", Defect and Defusion Forum, 388, 303-316.
15. Mallikarjuna B, Subba Bhatta S.H.C.V and Ramprasad S, (2021): "Velocity and thermal slip effects on MHD convective radiative two-phase flows in an asymmetric non-uniform channel", Propulsion and Power Research, 10, 169-179.
16. Srinivasacharya.D and Jagadeeshwar, (2019): "Effect of joule heating on the flow over an exponentially stretching sheet with convective boundary condition", Mathematical sciences, 13, 201-211.
17. Ali J. Chamkha, Dogonchi A.S and Ganji DD, (2019): "Magneto-hydrodynamic flow and heat transferof a hybrid nanofluidin a rotating system among two surfaces in the presence of thermal radiation and joule heating", AIP Advances 9, 025103.
18. Swain, B.K, Parida B.C, Kar. S and Senapati. N, (2020): "Viscous dissipation and joule heating effect on MHD flow and heat transfer past a stretching sheet embedded in a porous medium", Heliyon 6, e05338.
19. Umair Rashid, Azhar Iqbal, Haiyi Liang, Waris Khan, Muhammed Waqar, (2020): "Dynamics of water conveying zinc oxide through divergent-convergent channels with the effect of nanoparticles shape when Joule dissipation are significant", PLOS ONE, 16, (2021).
20. Kotnurkar, A., Kallolikar, N. (2022): Effect of Joule heating and entropy generation on multi-slip condition of peristaltic flow of Casson nanofluid in an asymmetric channel. *Journal of Biological Physics*, 48, 273-293.
21. Khashi'ie, N.S., Wahid, N.S., Md Arifin, N. et al. (2022): MHD stagnation-point flow of hybrid nanofluid with convective heated shrinking disk, viscous dissipation and Joule heating effects, Neural computing and applications 34, 17601-17613.

Printed by Pradip Kumar Chanda at The Indian Press Pvt. Ltd. 93A Lenin Sarani, Kolkata 700 013 and published by him for Books & Journals Pvt. Ltd. from 62 Lenin Sarani, Kolkata 700 013.